Lumped Parameter Models for Single- and Multiple–Layer Inductors

A. Massarini[1], M.K. Kazimierczuk[2], and G. Grandi[3]
[1]Dept. of Engineering Sciences, University of Modena, I-41100
[2]Dept. of Electrical Engineering, Wright State University, Dayton, OH 45435
[3]Dept. of Electrical Engineering, University of Bologna, I-40136

Abstract - A method for modeling inductors at high-frequency operation is presented. The method is based on analytical approaches which can predict turn inductances, turn-to-turn and turn-to-core capacitances using physical structure of windings. Turn inductances, turn-to-turn and turn-to-core capacitances of coils are then introduced into suitable lumped parameter equivalent circuits of inductors. The overall inductance and stray capacitance can be obtained through the use of the equivalent circuits. Both single- and multiple-layer inductors are considered. The method was tested with experimental measurements. The accuracy of the results was good in most cases. The derived expressions can be useful for the design of HF inductors and can also be used for simulation purposes.

I. Introduction

At high frequencies, the behavior of inductors and transformers is very different from their low frequency behavior. Skin and proximity effects cause the winding parasitic resistances to increase with the operating frequency, and the parasitic capacitances of the winding cannot be neglected, either. Hence, the overall reactance can be significantly affected by these phenomena. As a result, an accurate prediction of the response of inductors that operate at frequencies above several hundred kilohertz, such as, for instance, those used in high-frequency switching power converters and in EMI filters, is crucial for the design of such devices. The parasitic capacitances and resistances are distributed parameters which are negligible at low frequencies but play a role of increasing significance as the operating frequency increases. The inductance itself is not constant when the frequency changes. Thus, the theoretical prediction of the frequency response of an inductor is a difficult task.

The problem of high-frequency magnetic components is widely discussed in the literature, but mainly the aspects related to the parasitic ac winding resistances and losses in ferromagnetic cores have been addressed [1, 2, 3]. Some results concerning the stray capacitance of single-layer and multiple-layer coils are presented in [4, 5, 6]. More recently, a novel method suitable for the prediction of the overall stray capacitance of inductors has been presented [7]. The prediction of the overall inductance of coils is made through expressions based on simplified assumptions. These assumptions may not be satisfied in many windings used for high-frequency applications.

The aim of this paper is to propose a new method for deriving the overall inductance and stray capacitance of a single- or multiple-layer inductor, and compare the theoretical and experimental results. The method is based on a rigorous analytical approach used for the calculation of the turn inductances, and on an analytical simplified approach used for the calculation of the turn-to-turn and turn-to-core capacitances. Only the specification of the coil geometry is required. The lumped parameters obtained using the proposed methods allow us to derive the overall inductance and stray capacitance.

II. Models of the Inductor

Inductor windings have distributed parasitic parameters, which can be modeled in a simple way by a lumped parameter equivalent circuit shown in Fig. 1. It consists of an inductance L, a series ac resistance of the coil R_{ac}, and an overall stray capacitance C_s. In a more detailed model, each turn of the coil could be replaced by a lumped parameter circuit similar to that of Fig. 1. In this case, the inductance L should represent the self-inductance of the turn itself plus the contributions of mutual inductances due to all the other turns, whereas the shunt capacitance should be given by the contributions from the turn-to-turn and/or turn-to-core capacitances. The analysis is performed for cylindrical inductors made of a uniformly wound single wire.

0-7803-3500-7/96/$ 5.00 © 1996 IEEE

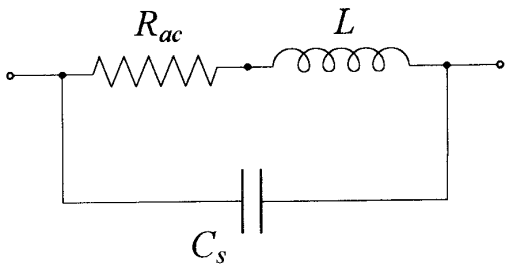

Figure 1: Basic lumped parameter circuit.

III. Inductance Calculation

Usually, the calculation of the inductance for a whole winding is performed using some ready-to-use expressions. These expressions have coefficients which are derived under the assumption that layers of turns can be replaced by a cylindrical shell in which the current is uniformly distributed. The coefficients are tabulated as a function of the winding geometry [8]. The approximation given by the above mentioned expressions for the predicted inductance may be poor in some cases, for instance when the number of turns is small or when there is some distance between turns. In order to improve the prediction of the inductance of a single- or multiple–layer winding, the detailed lumped parameter model can be used. The self- and mutual inductances of all the turns are required in this case. The overall inductance can be derived by means of a suitable combination of the self- and mutual inductances between turns.

A. *Mutual Inductances Calculation*

For the calculation of mutual inductances between the turns of an air-core inductor, the following expression (valid for circular coaxial turns) can be used [9]

$$M_{(i,j)(h,k)} \cong \cong \frac{\mu_0}{2}\int_0^{2\pi} \frac{R_i R_h cos\vartheta}{\sqrt{d_{j,k}^2 + R_i^2 + R_h^2 - 2R_i R_h cos\vartheta}} d\vartheta \quad (1)$$

where the left-hand side represents the mutual inductance between the j-th turn of the i-th layer and the k-th turn of the h-th layer, R_i and R_h are the turn radii of the i-th and the h-th layers, respectively. $d_{j,k}$ is the distance between the planes containing the j-th and the k-th turns (in the axial direction), ϑ is the angular coordinate around the turn, and μ_0 is the permittivity of vacuum. A cross-sectional view of a multiple-layer winding is shown in Fig. 2. The integral in (1) is an elliptic one. It can be solved through a numerical method or with the procedure described in the Appendix.

In the model proposed, an inductor made of N_l layers with N_t turns per layer has a total number of $(N_l N_t)^2$ self- and mutual inductances. Not all the mutual inductances are different from one another. In fact, $M_{(i,j)(h,k)} = M_{(h,k)(i,j)}$ and, furthermore, in both single- and multiple-layer coils, the periodicity of the geometrical structure results in a significant number of mutual inductances equal to one another. More precisely, between turns belonging to the same layer or to different layers, the mutual inductances do not change if the turns are equally shifted in the axial direction. Therefore, for a winding with N_l layers and N_t turns per layer,

$$M_{(i,j)(h,k)} = M_{(i,j+n)(h,k+n)} \quad (2)$$

where n is an integer, and

$$\begin{aligned} 1 \le j+n \le N_t \\ 1 \le k+n \le N_t. \end{aligned} \quad (3)$$

B. *Self-Inductances Calculation*

Self-inductances are the same for turns belonging to the same layer. They cannot be calculated using (1) with $i = h$ and $j = k$, but using the following expression [9]

$$M_{(i,j)(i,j)} = L_i \cong \mu_0 R_i \left(ln\frac{8R_i}{D_c/2} - \frac{7}{4} \right). \quad (4)$$

The turn radius R_i is the same for all the turns of the same layer. D_c indicates the diameter of the wire.

C. *Overall Inductance*

The global inductance can be derived under the assumption that the current flowing in the coil is the same for all turns. This assumption is true at low frequencies, yet it is valid at higher frequencies if currents through parasitic capacitances are negligible. The overall inductance is then given by

$$L = \sum_{i=1}^{N_l}\sum_{j=1}^{N_t}\sum_{h=1}^{N_l}\sum_{k=1}^{N_t} M_{(i,j)(h,k)}. \quad (5)$$

For a single-layer winding, $N_l = 1$. In this case, (2) and (4) become

$$M_{(1,j)(1,j+b)} = M_{(1,j+n)(1,j+b+n)} \quad (6)$$

$$M_{(1,j)(1,j)} = L_1. \quad (7)$$

Introducing (7) and (6) in (5), one obtains the overall inductance

$$L = \sum_{j=1}^{N_t} \sum_{k=1}^{N_t} M_{(1,j)(1,k)} =$$

$$= N_t L_1 + 2 \sum_{k=1}^{N_t - 1} (N_t - k) M_{(1,1)(1,k+1)}. \qquad (8)$$

The calculation of the self-inductance L_1 can be carried out by means of (4) with $i = 1$. Now, we have only $N_t - 1$ different mutual inductances which can be calculated as

$$M_{(1,1)(1,k+1)} = M_{1,k+1} =$$

$$= \frac{\mu_0}{2} \int_0^{2\pi} \frac{R_1^2 \cos\vartheta}{\sqrt{(kd)^2 + 2R_1^2(1 - \cos\vartheta)}} \, d\vartheta \qquad (9)$$

where d is the distance between planes containing adjacent turns.

The presence of a ferromagnetic core strongly affects self- and mutual inductances. An analytical approach is very difficult in this case, numerical methods of field analysis or experimental formulae are usually employed. Also the presence of a shield affects self- and mutual inductances. In fact, at high frequencies, the eddy-currents in the shield act as a magnetic screen thus decreasing the overall coil inductance. Skin and proximity effects in the wire slightly affect inductances if the ratio $2R_i/D_c$ is large enough. The case of small values of this ratio (inductors for high current applications) together with the other effects mentioned above, will be examined in detail in a further paper.

IV. Parasitic Capacitance Calculation

The total stray capacitance of inductors consists of the following components:

1. the turn–to–turn capacitances between turns of the same layer,
2. the turn–to–turn capacitances between turns of adjacent layers,
3. the turn-to-core capacitance, and the turn-to-shield capacitance.

A method for the calculation of the overall stray capacitance has been proposed in [7]. A brief review with some rearrangements of this method is reported here. The proposed method exploits winding symmetries in order to introduce basic cells for the calculation of the turn-to-turn capacitances. In Fig. 3, a basic cell $ABCD$ related to the turn-to-turn capacitance of a multiple-layer winding is

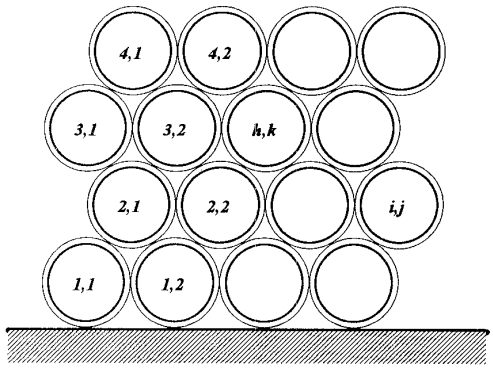

Figure 2: Cross-sectional view of a multiple-layer winding.

shown. The lines of the electric field $\mathbf{E}$ that get out from each turn fully surrounded by other conductors go to these conductors. No line can go either to other conductors or to infinity under the assumption that the conductors of the coil (turns, core, and shield) are close enough one to the others. Furthermore, because of symmetries in the winding geometry, all the turn-to-turn capacitances between adjacent turns must be equal. The elementary capacitance dC between two opposite corresponding elementary surfaces, dS, of two adjacent conductors can be expressed as

$$dC = \epsilon \frac{dS}{x} \qquad (10)$$

where $\epsilon = \epsilon_r \epsilon_0$ is the permittivity of a homogeneous medium and x is the length of a line of the electric field connecting two opposite elementary surfaces. The length x is not constant, but it is a function of the location of the elementary surface which, in turn, can be related to an angular coordinate θ.

V. Turn-to-Turn Capacitance

The basic cell suitable for the calculation of the turn-to-turn capacitances include a portion of the perimeter of the turn cross-section which corresponds to an angle of $\pi/3$ rad as shown in Fig. 3. Hence, in order to obtain the turn-to-turn capacitance, the elementary capacitance given by (10) must be integrated over the angle $\pi/3$.

In the basic cell, the lines of the electric field cross three regions: the insulating coatings of either turn and the air gap between them. The elementary capacitance dC between adjacent turns is, therefore, equivalent to the capac-

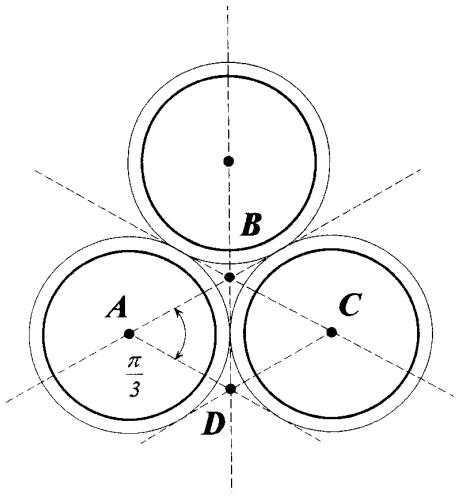

Figure 3: A basic cell $ABCD$ used for the calculation of the turn-to-turn capacitance.

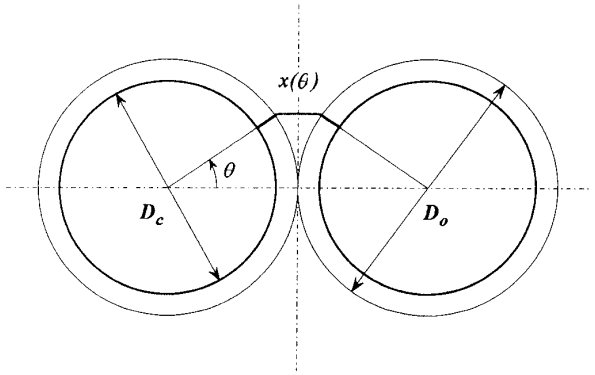

Figure 4: Assumed path $x(\theta)$ of an electric field line.

itance of a series combination of three elementary capacitors, each with a homogeneous dielectric material:

1. The insulating coating of a turn.
2. The air gap.
3. The insulating coating of an adjacent turn.

We are neglecting the presence of possible insulation between layers.

If the thickness of the insulating coating s is much lower than the outer diameter of the wire including insulation, D_o, we can approximate the paths of the electric field in the insulator by the insulator thickness s as shown in Fig. 4. It is more difficult to predict the paths of the electric field in the air gap between adjacent turns. The shortest possible paths are used for the calculation of the air-gap capacitance. These paths are segments parallel to the line that connects the centerlines of the turns under consideration. One of these segments is depicted in Fig. 4. This approximation can be considered as a conservative one for the design of HF inductors.

From the elementary capacitances of both the insulating coatings and the air gap, an equivalent elementary capacitance can be derived. Integration of this capacitance over the basic cell gives an expression for the turn-to-turn capacitance which is derived in the Appendix of [7]. The resulting expression seems not to be of practical use. Therefore, a simplified approach which leads to a more easy-to-use expression for the turn-to-turn capacitance is also provided by [7]. In the simplified approach, the basic cell is partitioned into three parts. Suitable border lines between the differents parts have been proposed. They are selected by means of an angle θ^* which is defined as the angle at which the elementary capacitance of the air gap equals the series combination of the elementary capacitances of the coatings. In each part, the series combination of the three elementary capacitances is approximated with the series combination of just the coating capacitances, or with the elementary capacitance of the air gap alone.

A. *Capacitance of the Insulating Coatings*

In Ref. [7], an expression for the coating capacitance was calculated starting from the capacitance of an elementary cylindrical shell of the insulating coatings. The following expression was obtained

$$C_c = \frac{2\epsilon_r\epsilon_0\theta^* l_t}{ln\frac{D_o}{D_c}} \tag{11}$$

where l_t is the turn length. However, under the assumption of small thickness s of the coatings, we do not introduce a significant error if we approximate the capacitance of the cylindrical shell with the capacitance of a parallel plane capacitor

$$C_c = \frac{\epsilon_r\epsilon_0\theta^* D_a l_t}{s}. \tag{12}$$

where $D_a = (D_o + D_c)/2$ is the average diameter of the insulating coating shell. In the part of the basic cell corresponding to $|\vartheta| \leq \vartheta^*$ in which the elementary capacitance of the air gap is larger, the equivalent capacitance is approximated by the series combination of just the coating capacitances. It is given by

$$C_{ttc} = \frac{C_c}{2} = \frac{\epsilon_r\epsilon_0\theta^* D_a l_t}{2s}. \tag{13}$$

B. *Capacitance of the Air Gap*

In the side parts of the basic cell corresponding to $\vartheta^* < |\vartheta| \leq \pi/6$ where the elementary capacitance of the air gap is smaller, the equivalent capacitance can be approximated by the capacitance of the air gap alone. Introducing in (10) the assumed path as a function of θ

$$x(\theta) = D_o(1 - cos\theta) \tag{14}$$

and the expression for an elementary surface dS, one can obtain the elementary air-gap capacitance

$$dC_g(\theta) = \epsilon_0 \frac{dS}{x(\theta)} = \epsilon_0 \frac{l_t D_o}{2x(\theta)} d\theta$$

$$= \epsilon_0 \frac{l_t D_o}{2D_o(1 - cos\theta)} d\theta = \epsilon_0 \frac{l_t}{2(1 - cos\theta)} d\theta. \tag{15}$$

Integrating this equation in the parts of the basic cell where the elementary capacitance of the air gap is smaller than the other elementary capacitances, one obtains

$$C_{ttg} = 2 \int_{\theta^*}^{\pi/6} \frac{\epsilon_0 l_t}{2(1 - cos\theta)} d\theta$$

$$= \epsilon_0 l_t \int_{\theta^*}^{\pi/6} \frac{1}{1 - \cos\theta} \, d\theta$$

$$= \epsilon_0 l_t \left[\cot\left(\frac{\theta^*}{2}\right) - 3.732 \right]. \tag{16}$$

C. *Total Capacitance of the Basic Cell*

The total capacitance of the basic cell is obtained by adding the contributions from its parts

$$C_{tt} = C_{ttc} + C_{ttg}$$

$$= \epsilon_0 l_t \left[\epsilon_r \frac{D_a \, \theta^*}{2s} + \cot\left(\frac{\theta^*}{2}\right) - 3.732 \right] \tag{17}$$

where θ^* is given by

$$\theta^* = \arccos\left(1 - \frac{2s}{\epsilon_r D_a}\right). \tag{18}$$

In this paper, θ^* is derived using (12) instead of (11) as in [7].

VI. Turn-to-Core Capacitance

A similar approach can also be used to calculate the turn-to-core and/or the turn-to-shield capacitances. Now we are neglecting the presence of a possible insulation between the first layer and the core. Assuming that the core is a conductor plane of symmetry as depicted in Fig. 5, the path lengths of the electric field lines between a turn and the plane conductor are one half the path lengths between adjacent turns. The turn-to-core basic cell considered for the calculation of the capacitance should be wider than the turn-to-turn basic cell. In fact, a portion of the turn cross-section perimeter which corresponds to an angle of $\pi/2$ is included in the turn-to-core basic cell, as it can be seen from Fig. 2. Nevertheless, as a first approximation all the basic cells can be assumed identical. Therefore,

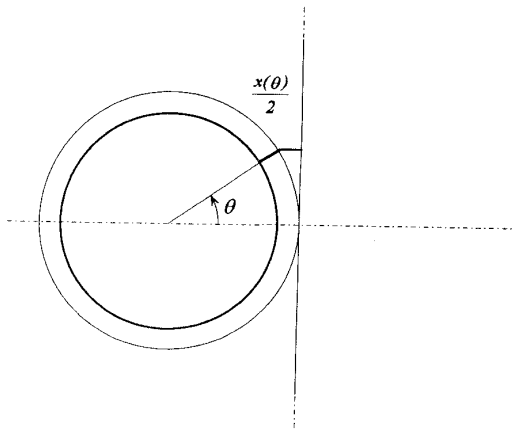

Figure 5: Assumed path of the electric field line between a turn and a conductive core.

$$C_{tc} \cong 2C_{tt}. \tag{19}$$

VII. Overall Stray Capacitance

In order to determine the stray capacitance of a winding as depicted in Fig. 1, a network consisting of lumped capacitors is solved. A network of lumped capacitors obtained for a single-layer coil wound on a conductive core is shown in Fig. 6. The simplest case concerns a single-layer winding of n turns with no core and/or shield. For this winding, the total stray capacitance is given by the equivalent capacitance of $n - 1$ turn-to-turn capacitances in series

$$C_s = \frac{C_{tt}}{n - 1}. \tag{20}$$

Unfortunately, in this case the assumptions made in the previous sections are not well satisfied and, therefore, the accuracy of (20) is not very good. It decreases with increasing number of turns and increasing length-to-diameter ratio of the winding. A better approach to the calculation of the stray capacitance of single-layer coreless inductors is presented in [10].

For a single-layer coil consisting of n turns wound on a conductive core, a lumped capacitor network similar to

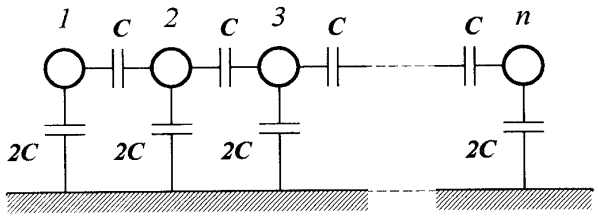

Figure 6: Lumped capacitor network for a single-layer coil with conductive core.

that depicted in Fig. 6 must be solved. The equivalent capacitance between the first and the last turn of the winding does not depend on the number of turns when it equals or exceeds 10. It is given by

$$C_s = 1.366\, C_{tt}, \quad \text{for} \quad n \geq 10. \tag{21}$$

A more detailed derivation of (21) is provided in [7].

For two-layer coreless coils, under the assumptions that the outer layer is wound in the opposite direction of the inner one, the stray capacitance is given by

$$C_s = 1.618 C_{tt}, \quad \text{for} \quad n \geq 10. \tag{22}$$

Under the previous assumptions, and when also a conductive core or shield is present, the overall stray capacitance of a two-layer coil is given by

$$C_s = 1.83 C_{tt}, \quad \text{for} \quad n \geq 10. \tag{23}$$

It can be seen that two-layer coils are affected by a higher stray capacitance than single-layer coils. They are also affected by a higher resistance at high-frequency operation [3]. Thus, in general, using multiple-layer coils is not a good practice for inductors designed for high-frequency operation.

VIII. Comparison of Predicted and Measured Results

The results given by the proposed method have been compared with those measured for several inductors. Some illustrative examples are given in this section. As a first example the inductance of four single-layer coils for EMI filtering applications was calculated and compared with experimental measurements. All the coils were made with a single wire having a diameter $D_c = 1.4$ mm. The radius of the turns was $R = 39.75$ mm in all cases with the exception of the 80-turn coil for which $R = 40.6$ mm. The inductances predicted by the method proposed in Section III-C along with the values measured at 1 kHz are reported in the Table I.

Table I. Calculated and Measured Inductances

N_t (turns)	d (mm)	Calculated $L(\mu\text{H})$	Measured $L(\mu\text{H})$
38	1.84	83.9	84.1
47	2.66	85.2	85.6
50	3.01	83.6	84.7
80	1.66	243.4	244.6

The comparison of the calculated and measured results shows a good agreement.

As an example for the prediction of the stray capacitance, a single-layer winding inductor with a powder iron core for high-frequency power converters was considered. The coil had 95 circular turns of $R_1 = 7.15$ mm diameter. The wire had an outer diameter $D_o = 0.495$ mm with an inner diameter of the conductor $D_c = 0.45$ mm (coating thickness $s = 0.0225$ mm.) The dielectric constant of the coating material was $\epsilon_r = 3.5$. From (18), one obtains

$$\theta^* = \arccos\left(1 - \frac{2 \times 0.0225}{3.5 \times 0.4725}\right) = \\ = 0.2338 \text{ rad} = 13.4°. \tag{24}$$

Substituting this into (17) yields

$$C_{tt} = 8.85 \times 10^{-12} \times \pi \times 14.3 \times 10^{-3} \\ \times \left[3.5 \times \frac{0.4725 \times 0.2338}{2 \times 0.0225} + cot\left(\frac{0.2338}{2}\right) - 3.732\right] = \\ = 5.318 \text{ pF}. \tag{25}$$

Substitution of $C_{tt} = 5.318$ pF into (21) gives

$$C_s = 1.366 \times 5.318 = 7.26 \text{ pF}. \tag{26}$$

Using this value, the calculated self-resonant frequency of the inductor, which had an inductance $L = 75$ μH at 100 Hz, was 6.8 MHz. The self-resonant frequency measured with an HP4194A impedance/gain-phase analyzer was 6.2 MHz. The corresponding total stray capacitance was 8.78 pF. The error in determining the first self-resonant frequency f_{s1} was

$$\frac{\Delta f_{s1}}{f_{s1}} \times 100\% = \frac{6.8 - 6.2}{6.2} \times 100\% = 9.68\%. \tag{27}$$

Therefore, the error of determining the self-capacitance was

$$\frac{\Delta C_s}{C_s} \times 100\% = \frac{7.26 - 8.78}{8.78} \times 100\% = -17.3\%. \tag{28}$$

IX. Conclusions

A method for predicting the inductance and the stray capacitance of inductor windings has been proposed herein. The derived equations can be used for designing and modeling inductors which operates at high frequencies. The expression for the inductance is derived analytically through all self- and mutual inductances of turns. The expression for the stray capacitance is obtained with a simplified analytical approach and is simple enough so that a pocket calculator can be used. The proposed approach is also suitable for predicting the first self-resonant frequency of both single- and multiple-layer inductors. Physical insight into the influence of the number of layers and the number of turns per layer on the inductor parameters is provided.

References

[1] P. L. Dowell, "Effects of Eddy Currents in Transformer Windings," *Proc. IEE*, Vol. 113, No. 8, pp. 1287–1394, August 1966.

[2] M. K. Jutty, V. Swaminathan, and M. K. Kazimierczuk, "Frequency Characteristics of Ferrite Core Inductors," *Proc. Electrical Manufacturing & Coil Winding Symposium*, pp. 369–372, Chicago, IL, 1993.

[3] M. Bartoli, A. Reatti, and M. K. Kazimierczuk, "Modeling Iron-Powder Inductors at High Frequencies," *Proc. Industry Applications Conf.*, Vol. 2, pp. 1225–1232, Denver, CO, 1994.

[4] E. C. Snelling, *Soft Ferrites, Properties and Applications*, ILIFFE BOOKS Ltd.: London, 1969.

[5] W. T. Duerdoth, "Equivalent Capacitances of Transformer Windings," *Wireless Engr.*, 23, p. 161, 1946.

[6] R. G. Medhurst, "H. F. Resistance and Self-Capacitance of Single-Layer Solenoids," *Wireless Engr.*, 24, p. 35, 1947.

[7] A. Massarini and M. K. Kazimierczuk, "Modeling the Parasitic Capacitance of Inductors," *Proc. of 16th Capacitor and Resistor Technology Symposium (CARTS 96)*, New Orleans, Mar. 1996, pp. 78-85.

[8] F. W. Grover, *Inductance Calculations*, Van Nostrand: New York (USA), 1946.

[9] E. Durand, *Magnétostatique*, MASSON: Paris, 1968.

[10] G. Grandi, M. K. Kazimierczuk, A. Massarini, and U. Reggiani "Stray Capacitances of Single-Layer Air-Core Inductors for High Frequency Applications," *accepted at IAS 96 Conf.*, San Diego, CA, Oct. 1996.

[11] E. Janke, and F. Emde, *Tables of Functions with Formulae and Curves*, DOVER: New York, 1945.

Appendix

The elliptic integral in (1) can be calculated without much difficulties through usual numerical integration procedures. Alternatively, it can be reduced to the form

$$M_{(i,j)(h,k)} = \mu_0 \sqrt{R_i R_h} \left[\left(\frac{2}{c} - c \right) I_1(c) - \frac{2}{c} I_2(c) \right] \quad (29)$$

where

$$c^2 = \frac{4 R_i R_h}{d_{j,k}^2 + (R_i + R_h)^2}. \quad (30)$$

The functions I_1 and I_2 are the Legendre's elliptic integrals of the first and second kinds. They are built-in functions in the main mathematical libraries and are also available in the format of tables or graphs in many mathematical handbooks [11]. They are given by

$$I_1(c) = \int_0^{\pi/2} \frac{1}{\sqrt{1 - c^2 sen^2 \psi}} \, d\psi = $$

$$= \frac{\pi}{2} \left[1 + \sum_{n=1}^{\infty} \left(\frac{(2n-1)!!}{(2n)!!} \right)^2 c^{2n} \right] \quad (31)$$

and

$$I_2(c) = \int_0^{\pi/2} \sqrt{1 - c^2 sen^2 \psi} \, d\psi = $$

$$= \frac{\pi}{2} \left[1 - \sum_{n=1}^{\infty} \left(\frac{(2n-1)!!}{(2n)!!} \right)^2 \frac{c^{2n}}{(2n-1)} \right]. \quad (32)$$